

# Three-dimensional diabetic macular edema thickness maps based on fluid segmentation and fovea detection using deep learning

Jing-Jing Xu<sup>1</sup>, Yang Zhou<sup>2</sup>, Qi-Jie Wei<sup>2</sup>, Kang Li<sup>3</sup>, Zhen-Ping Li<sup>3</sup>, Tian Yu<sup>3</sup>, Jian-Chun Zhao<sup>2</sup>, Da-Yong Ding<sup>2</sup>, Xi-Rong Li<sup>4</sup>, Guang-Zhi Wang<sup>1</sup>, Hong Dai<sup>3</sup>

<sup>1</sup>School of Medicine, Tsinghua University, Beijing 100084, China

<sup>2</sup>Visionary Intelligence Company Limited, Beijing 100872, China

<sup>3</sup>Department of Ophthalmology, Beijing Hospital, National Center of Gerontology, Institute of Geriatric Medicine, Chinese Academy of Medical Sciences, Beijing 100730, China

<sup>4</sup>Key Lab of Data Engineering and Knowledge Engineering, Renmin University of China, Beijing 100872, China

**Correspondence to:** Hong Dai. Department of Ophthalmology, Beijing Hospital, National Center of Gerontology, Institute of Geriatric Medicine, Chinese Academy of Medical Sciences, Beijing 100730, China. dai-hong@x263.net

Received: 2021-07-19 Accepted: 2021-11-09

## Abstract

• **AIM:** To explore a more accurate quantifying diagnosis method of diabetic macular edema (DME) by displaying detailed 3D morphometry beyond the gold-standard quantification indicator-central retinal thickness (CRT) and apply it in follow-up of DME patients.

• **METHODS:** Optical coherence tomography (OCT) scans of 229 eyes from 160 patients were collected. We manually annotated cystoid macular edema (CME), subretinal fluid (SRF) and fovea as ground truths. Deep convolution neural networks (DCNNs) were constructed including U-Net, sASPP, HRNetV2-W48, and HRNetV2-W48+Object-Contextual Representation (OCR) for fluid (CME+SRF) segmentation and fovea detection respectively, based on which the thickness maps of CME, SRF and retina were generated and divided by Early Treatment Diabetic Retinopathy Study (ETDRS) grid.

• **RESULTS:** In fluid segmentation, with the best DCNN constructed and loss function, the dice similarity coefficients (DSC) of segmentation reached 0.78 (CME), 0.82 (SRF), and 0.95 (retina). In fovea detection, the average deviation between the predicted fovea and the ground truth reached  $145.7 \pm 117.8 \mu\text{m}$ . The generated macular edema thickness

maps are able to discover center-involved DME by intuitive morphometry and fluid volume, which is ignored by the traditional definition of  $\text{CRT} > 250 \mu\text{m}$ . Thickness maps could also help to discover fluid above or below the fovea center ignored or underestimated by a single OCT B-scan.

• **CONCLUSION:** Compared to the traditional unidimensional indicator-CRT, 3D macular edema thickness maps are able to display more intuitive morphometry and detailed statistics of DME, supporting more accurate diagnoses and follow-up of DME patients.

• **KEYWORDS:** diabetic macular edema; fluid segmentation; fovea detection; 3D macular edema thickness maps; deep learning

**DOI:10.18240/ijo.2022.03.19**

**Citation:** Xu JJ, Zhou Y, Wei QJ, Li K, Li ZP, Yu T, Zhao JC, Ding DY, Li XR, Wang GZ, Dai H. Three-dimensional diabetic macular edema thickness maps based on fluid segmentation and fovea detection using deep learning. *Int J Ophthalmol* 2022;15(3):495-501

## INTRODUCTION

According to the ninth edition of the global diabetes atlas from the International Diabetes Federation (IDF) in 2019, there were 463 million of people with diabetes in the world, and 116.4 million in China<sup>[1]</sup>. Li *et al*<sup>[2]</sup> showed that prevalence of diabetes among adults living in China was 12.8% using 2018 diagnostic criteria from the American Diabetes Association. Diabetic retinopathy is one of the most common and serious complications of diabetes<sup>[3]</sup>, in which diabetic macular edema (DME) is the main cause of visual impairment or even complete loss in diabetic patients<sup>[4]</sup>.

The measurement of macular edema is critical for the diagnosis and treatment of DME. Measured by optical coherence tomography (OCT), central retinal thickness (CRT) is the gold standard for quantitative evaluation of DME. In the guidelines from the European Retinal Society in 2017 and the American Ophthalmology Society in 2020, CRT is an important indicator for DME severity and treatment response<sup>[5-6]</sup>. Center-involved

**Table 1 Information of datasets for training, validation, and testing**

Parameters	Training set			Validation set			Testing set		
	Patients	Eyes	Annotated B-scans	Patients	Eyes	Annotated B-scans	Patients	Eyes	Annotated B-scans
Fluid segmentation	87	125	426	36	47	143	37	57	162
Fovea detection	87	125	125	36	47	47	37	57	57

DME (CI-DME) is defined as CRT of more than 250  $\mu\text{m}$  and requires anti-VEGF treatment<sup>[6]</sup>.

However, as a unidimensional indicator (the retinal thickness across the fovea center), CRT is insufficient to present overall morphological changes of macula. Fluid is actually observed in some patients with normal CRT ( $<250 \mu\text{m}$ , according to the definition of CI-DME) and require treatments, indicating the limitation of CRT as an indicator. Furthermore, given that retina is a three-dimensional (3D) tissue, an OCT B-scan only shows a cross section of retina, which may leave the fluid on other cross sections ignored or underestimated. More effective approaches are required to improve the accuracy of DME diagnosis for better treatments.

We propose the concept of 3D macular edema thickness maps. We performed fluid segmentation and fovea detection using a deep convolution neural network (DCNN) called HRNetV2-W48, based on which we calculated the volume and average thickness of retina, cystoid macular edema (CME) and subretinal fluid (SRF) separately on the Early Treatment Diabetic Retinopathy Study (ETDRS) grid of fundus photograph to generate thickness maps. Compared to traditional indicators, macular edema thickness maps are able to support more accurate diagnoses by presenting the 3D morphometry of fluid (CME and SRF), and have the potential to be applied in follow-up of DME patients.

## SUBJECTS AND METHODS

**Ethical Approval** The images used in the research were provided by Beijing Hospital. This study received formal review and approval from the Ethics Committee of Beijing Hospital and adhered to the tenets of the Declaration of Helsinki.

**Dataset** A total of 229 completely anonymized OCT cube scans (Spectralis OCT, Heidelberg Engineering, Heidelberg, Germany) of 229 eyes from 160 patients affected by DME were collected consecutively from Department of Ophthalmology, Beijing Hospital since 2010. Inclusion criteria: patients diagnosed as DME based on history of diabetes, fundus photograph and OCT scans. Exclusion criteria: patients with other retinal diseases (*e.g.*, age-related macular degeneration, retinal vein occlusion or retinal breaks); patients with incomplete OCT scans or unsatisfied image quality (*e.g.*, off-center, blocked signal or missing signal). Each cube scan includes 25 consecutive B-scans. The image resolution of each B-scan is  $512 \times 496$  pixels, covering a scanning field of  $20^\circ \times 20^\circ$  (approximately  $6 \times 6 \text{ mm}^2$ ).

OCT images were randomized into training set (125 eyes), validation set (47 eyes), and testing set (57 eyes) with a ratio of approximately 2:1:1 of patients (Table 1). In the fluid segmentation task, three to five B-scans with visible fluid were selected for manual annotation. Internal limiting membrane (ILM), retinal pigment epithelium (RPE), CME, SRF were manually annotated by trained ophthalmologists at pixel-level in each B-scan. Contrast limited adaptive histogram equalization, a method of image enhancement, was applied to help ophthalmologists recognize the boundary of fluid. In the fovea detection task, only one B-scan was selected and annotated with foveal coordinates in each cube scan.

A consensus grading program and a review system were performed after manual annotation. The training set was annotated by a single ophthalmologist. The testing set was annotated independently by two ophthalmologists and then reviewed by a supervisor.

## 3D Macular Edema Thickness Maps Calculating Workflow

The architecture of workflow is illustrated in Figure 1. To obtain macular edema thickness maps, three main modules are embedded: 1) macular fluid segmentation module (DCNN), 2) macular fovea detection module (DCNN), 3) macular edema thickness map generation module. Given a cube of OCT B-scans, the fluid segmentation module predicts the retinal region and edema region. Meanwhile, the macular fovea detection module predicts foveal coordinates. Subsequently, in the macular edema thickness map generation module, the fluid region and foveal coordinates in OCT are mapped onto the colored fundus photograph based on the positional correspondence relationship. Finally, 3D macular edema thickness maps with ETDRS grid are obtained.

**Macular fluid segmentation module** A DCNN of HRNetV2-W48+Object-Contextual Representation (OCR) architecture<sup>[7-9]</sup> was used in the segmentation module. There are 25 B-scans in one cube. This module takes B-scan as input, resizes each B-scan to  $512 \times 512$ , and determines whether each pixel belongs to CME, SRF, retina or background.

In the training process, data augmentation was used to increase the generalization ability, including random horizontal flipping, rotation, random cropping and aspect ratio changing. The maximum number of training epochs was 100. The learning rate was divided by 10 if the performance did not improve in 10 consecutive epochs. Once the rate reached  $10^{-8}$ , early stop occurred.

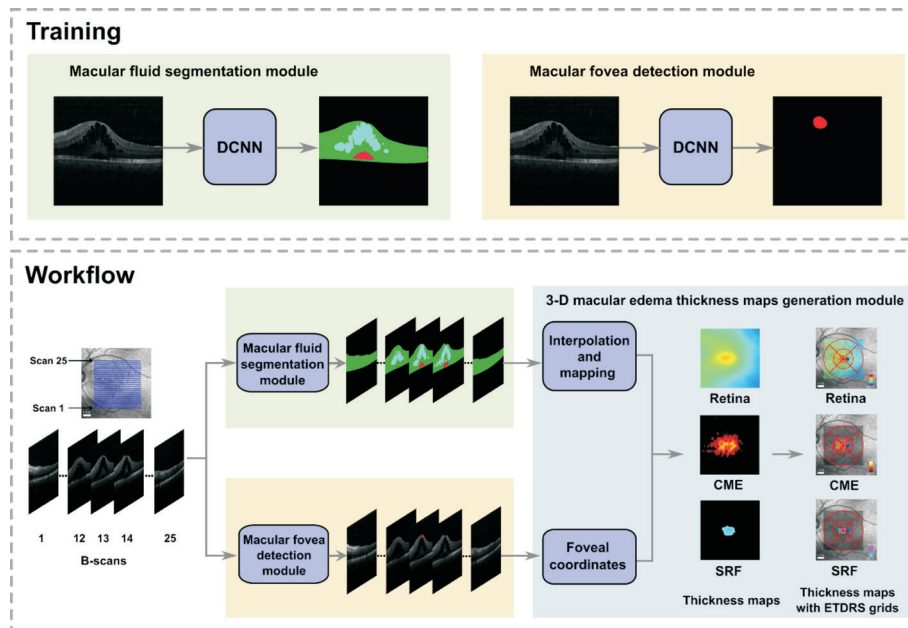


**Figure 1 Training of macular fluid segmentation module and macular fovea detection module, and workflow of 3D macular edema thickness maps generation** Red dot: Predicted fovea center; Blue dot: Scan center.

To reach the best performance, we compared following DCNNs: 1) U-Net. Most of the existing fluid segmentation literature used U-Net<sup>[10-12]</sup> or its variants<sup>[13-16]</sup> as the segmentation network. 2) sASPP. Hu *et al*<sup>[17]</sup> proposed stochastic atrous spatial pyramid pooling (sASPP) method based on Deeplabv3+<sup>[18]</sup>, which improved the performance and stability of fluid segmentation. 3) HRNetV2-W48, HRNetV2-W48+OCR, and HRNetV2-W48+OCR (WDice). In recent years, HRNet and its variant HRNet+OCR showed excellent performance in natural scene segmentation tasks<sup>[7-9]</sup>.

As common practice, dice similarity coefficient (DSC) was applied as the performance metric. Its definition is

$$DSC = \frac{2|X \cap Y|}{|X| + |Y|} = \frac{2TP}{2TP + FP + FN}$$

where X is the segmentation result and Y is the ground truth. TP represents the number of true positives. FP is the false positives, and FN is the false negatives.

The network was implemented by PyTorch (V1.6.0) framework and Python (V3.7.7). The experimental environment was Linux OS and hardware of Intel(R) Core(TM) i7-6850K CPU @ 3.60GHz, GeForce GTX 1080 Ti.

**Macular fovea detection module** The network backbone, training process and environment configuration of macular fovea detection module were the same as the retinal fluid segmentation module. Like Liefers *et al*<sup>[19]</sup>, a circle with a radius of 20 pixels around the manually annotated macular fovea center was set as the ground truth. The data augmentation only contained random horizontal flipping.

Every B-scan of one cube was fed into the network and the probability of fovea of each pixel was calculated. Two hundred

pixels with highest probability were selected as candidate points. Then the candidate points with probability lower than a prescribed threshold were removed. Eventually, foveal coordinates were determined by the mean coordinates of reserved candidate points.

**Macular edema thickness maps generation module** Each cube includes 25 consecutive B-scans. Through the two modules above, the fluid in each B-scan was segmented, and the fovea in each cube was detected. The thickness of macular edema was measured from segmentation results and mapped on the fundus photograph to generate thickness maps of CME, SRF and retina using bilinear interpolation algorithm (Figure 2). And then the foveal coordinates were mapped onto the fundus photograph. Thickness maps were divided by the ETDRS grid into central fovea (1-mm diameter), parafovea (1-3 mm), and lateral macular area (3-6 mm). The middle ring and the outer ring of the grid were further divided into 4 quadrants: superior, inferior, nasal, and temporal. The volume and average thickness of retina, CME and SRF in different zones could be calculated separately (Figure 2).

Sometimes, the cube scan center deviated from the center of the macula because of eccentric fixate or actual scanning requirements. To match the position of ETDRS grid, an offset should be considered. If part of the ETDRS grid was not covered by the cube scan, it would be estimated by bilinear interpolation algorithm.

## RESULTS

**Fluid Segmentation** First we compared the performance of different DCNNs, in which the cross entropy was as the loss function (Table 2). The best backbone was selected. Then

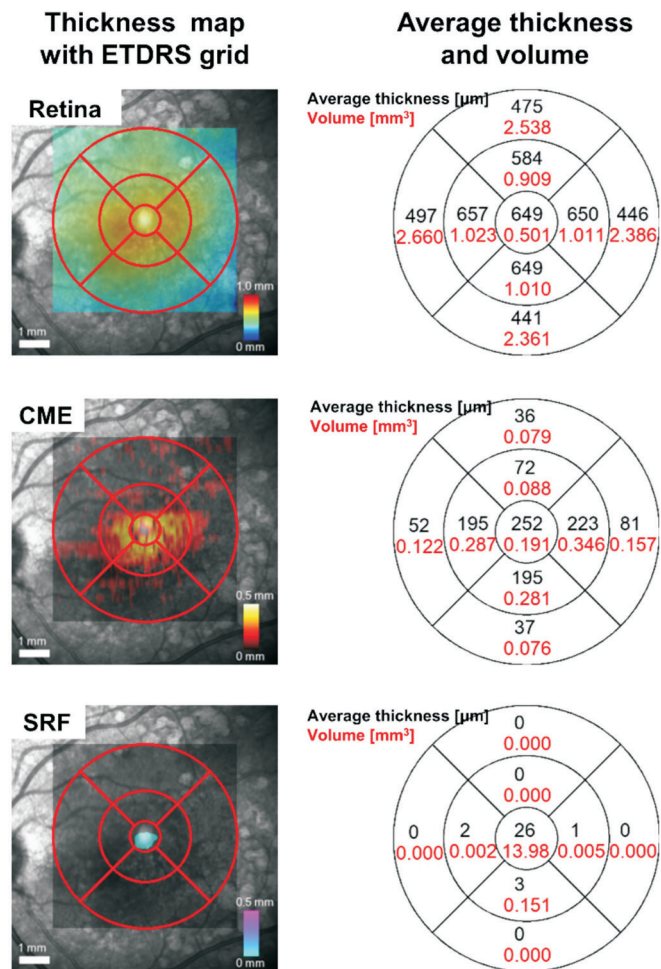


**Figure 2** An example of 3D macular edema thickness maps with ETDRS grid. Red font shows the volume ( $\text{mm}^3$ ) and black font shows the average thickness ( $\mu\text{m}$ ) of each grid zone.

**Table 2** DSC of fluid, CME, SRF, and retina in different DCNNs

DCNNs	Fluid	CME	SRF	Retina
U-Net	0.66	0.70	0.63	0.94
sASPP	0.74	0.71	0.76	0.95
HRNetV2-W48	0.76	0.74	0.77	0.95
HRNetV2-W48+OCR	0.77	0.75	0.78	0.95
HRNetV2-W48+OCR (WDice)	0.80	0.78	0.82	0.95

DCNN: Deep convolution neural network; CME: Cystoid macular edema; SRF: Subretinal fluid; OCR: Object-Contextual Representation.

different loss functions (CE, CE with weights, binary CE, Dice, Dice with weights) were compared to select the loss function with best performance.

The DSC of CME, SRF, and retina was calculated on the test dataset. The DSC of fluid (mean of CME and SRF) was used to compare different experiments more intuitively. HRNetV2-W48+OCR trained with weighted Dice loss function had the best performance in all DCNNs. In most networks, the DSC of SRF is usually higher than of CME. A possible explanation is that usually SRF has a clearer boundary in B-scans than CME and is thus easier to be recognized.

**Fovea Detection** The average deviation of fovea detection is as short as  $145.7 \mu\text{m}$  ( $\pm 117.8 \mu\text{m}$ ). Given the foveal diameter is typically 1.0-1.5 mm, more than 98% (56/57 cases of the testing set) of the deviation distances are within 0.5 mm from the fovea center, indicating a satisfactory fovea detection.

**Generation of 3D Macular Edema Thickness Map and Its Clinical Applications** Based on automated fluid segmentation and fovea detection, thickness maps of CME, SRF and retina were generated, and divided by ETDRS grid (Figure 2). This retinal thickness map shows the topography of macula, while CME thickness map and SRF thickness map show the thickness and distribution of intraretinal and subretinal fluid separately in the fundus photograph, whose 3D display is more intuitive to evaluate the severity of macular edema than CRT, the traditional unidimensional indicator. In the nine zones of ETDRS grid, the volume and average thickness of retina, CME and SRF in different zones could be calculated separately (Figure 2).

Compared to mere OCT B-scans and CRT (traditional indicator), our 3D macular edema thickness maps are more intuitive to display the distribution and thickness of macular edema and its distance to the fovea, and thereby better evaluate the severity of macular edema. Center-involved DME is defined as CRT of more than  $250 \mu\text{m}$ . Figure 3 shows four cases with normal CRT ( $< 250 \mu\text{m}$ ), but fluid in the central zone is observable in thickness maps, indicating the superiority of thickness maps upon CRT in diagnoses. Furthermore, when evaluated by a single OCT B-scan, fluid above or below the fovea center might be ignored or underestimated, while are observable in thickness maps (Figure 4). In these cases, thickness maps are more intuitive and accurate to evaluate the distribution and severity of edema.

We applied follow-up thickness maps for DME patients before and after anti-vascular endothelial growth factor (anti-VEGF) treatment. Changes of CME, SRF, and retinal thickness in the four-month follow-up were summarized from thickness maps, providing more details for clinical evaluations than simple CRT. The anti-VEGF treatments were performed in months 2, 3 and 4. We demonstrated changes of average CME, SRF and retinal thickness in the central 1 mm (Figure 5). Compared to simple CRT, thickness maps are able to display CME and SRF thickness individually and exclusively from retinal tissues.

**DISCUSSION**

A lot of traditional methods and networks have been applied in macular fluid segmentation based on OCT. Breger *et al*<sup>[20]</sup>, Samagaio *et al*<sup>[21]</sup>, and Jemshi *et al*<sup>[22]</sup> applied traditional methods to detect macular edema. However, studies from Schlegl *et al*<sup>[23]</sup>, Lee *et al*<sup>[11]</sup>, Roy *et al*<sup>[13]</sup>, Hu *et al*<sup>[17]</sup>, Bogunovic *et al*<sup>[24]</sup>, Guo *et al*<sup>[14]</sup>, Liu *et al*<sup>[15]</sup> showed that DCNNs achieved better performance in fluid segmentation task compared

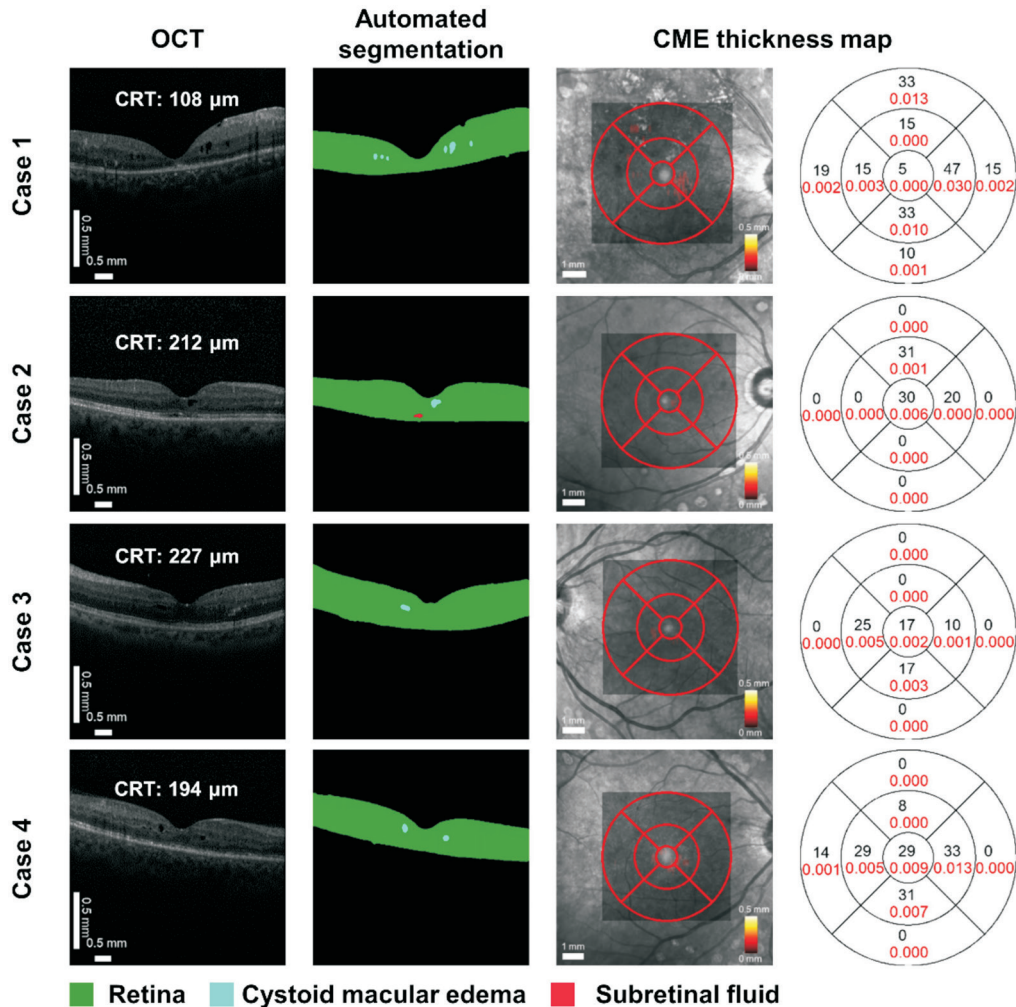


Figure 3 DME cases with normal CRT (<250  $\mu\text{m}$ , incorrectly defined as normal by CRT), indicating the limitation of CRT Red font shows the volume ( $\text{mm}^3$ ) and black font shows the average thickness ( $\mu\text{m}$ ) of each grid zone.

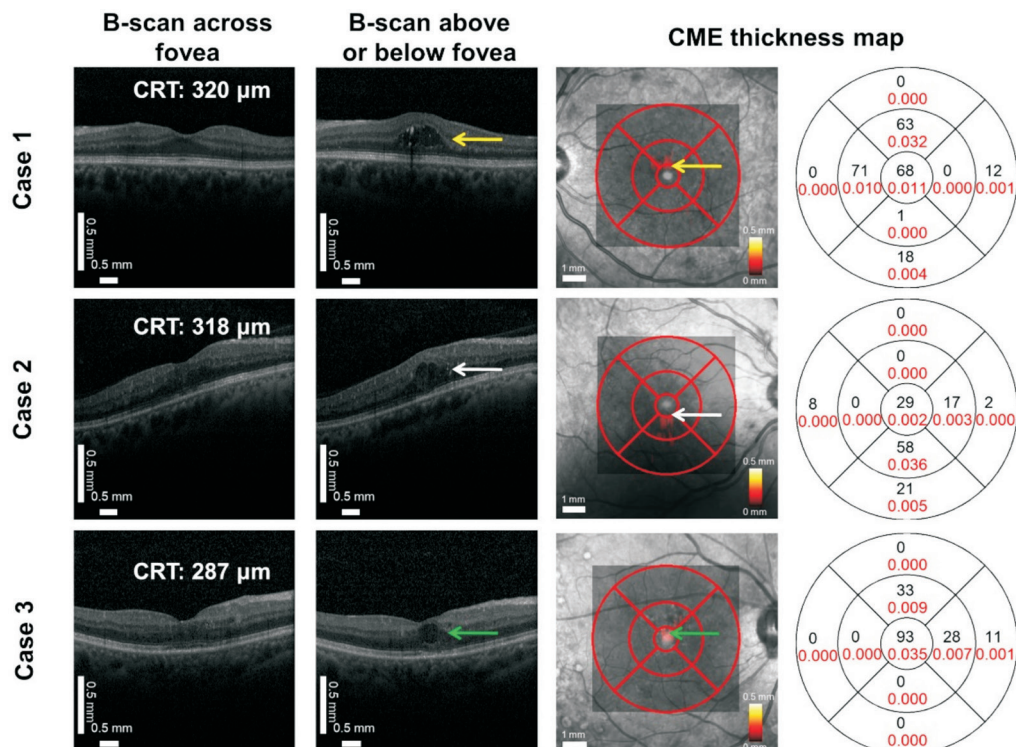
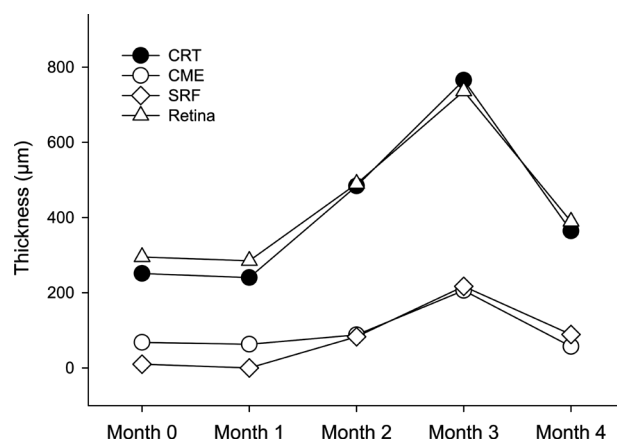


Figure 4 DME cases with observable fluid in CME thickness map (and in B-scans above or below the fovea center) might be ignored by a single OCT B-scan across the center Red font shows the volume ( $\text{mm}^3$ ) and black font shows the average thickness ( $\mu\text{m}$ ) of each grid zone.



**Figure 5** Changes of CME, SRF, and retinal thickness in the central 1 mm along the four-month follow-up summarized from thickness maps.

with traditional methods. Most of the existing literature used U-Net or its variants as the segmentation network. Hu *et al*<sup>[17]</sup> proposed sASPP method based on Deeplabv3+, which improved the performance and stability of fluid segmentation comparing to 2D and 3D U-net. In recent natural scene segmentation, HRNet and its variant HRNet+OCR showed excellent performance<sup>[7-9]</sup>. We compared the performance of different networks. HRNetV2-W48+OCR showed the best performance in different kinds of edema and fluid compared to U-Net, sASPP, and HRNetV2-W48, and only failed in images of poor-quality or with artifacts.

In cases of macular edema, the retina usually loses its structure, which leads to biases in fovea detection in most OCT devices. Niu *et al*<sup>[25]</sup> detected the fovea successfully in normal eyes and AMD patients based on changes in retinal thickness but failed in cases of macular edema. Wu *et al*<sup>[26]</sup> segmented the retina according to the graph theory method, detected the fovea according to thickness of the optic nerve fiber layer, and got an average deviation of 162.3 µm in CME caused by branch retinal vein occlusion (BRVO) and central retinal vein occlusion (CRVO), which is close to our results in DME patients (145.7±117.8 µm). Liefers *et al*<sup>[19]</sup> first proposed a deep learning method for fovea detection by identifying the marked area of 60×20 µm<sup>2</sup> around the fovea as a segmentation task, and obtained an average deviation of 215 µm in DME patients. Different from methods above, we applied HRNetV2-W48 to detect the fovea and achieved a higher accuracy.

In 1991, ETDRS proposed a fast macular topography to calculate average retinal thickness and volume in nine zones, which is called ETDRS grid and widely applied in current OCT devices. However, errors occur in automatic prediction of the fovea and retina structures in cases of macular edema. In our study, we propose the concept of macular edema thickness map, and calculate the volume and average thickness of retina,

CME and SRF separately on the ETDRS grid. Compared to the traditional evaluation method of observing OCT B-scans directly, 3D macular edema thickness maps present distribution of the intraretinal and subretinal fluid more intuitively and present the volume and average thickness of different types of edema in each grid zone. The average thickness of the central CME and SRF might be more sensitive compared to CRT as indicators in follow-ups, which requires further exploration. 3D macular edema thickness maps of patients will help doctors in treatment strategies, evaluation of treatment effects, and the timing of retreatment. In future studies, we would also include diffuse macular edema, hard exudation, *etc.* in the assessment of macular edema, and even include macular edema caused by other diseases such as BRVO and CRVO.

The current study still has several limitations. The amount of data in this study was small. The images in the test set and training set were from only one OCT device. In further study we could try to expand the dataset and include other devices. The current network only had a good performance in clear OCT images, showing significant errors in images with poor clarity due to cataracts, vitreous turbidity, artifacts, *etc.* The network needs further improvement and optimization. This research only included images of DME patients. Further study could collect images of macular edema caused by BRVO, CRVO and other diseases, to test the performance of the current network. Macular edema includes not only cystoid macular edema and subretinal fluid, but also sponge-like diffuse retinal thickening, hard exudation and other manifestations. Currently our network is not able to identify those kinds of lesions. 3D macular edema thickness maps and calculation of the fluid volume and average thickness are based on the cube mode in the OCT device. The construction of 3D macular edema thickness maps based on other scanning modes (such as star scans) needs further study.

In summary, we developed a deep learning network with better performance in macular fluid segmentation and fovea detection, based on which we generated 3D macular edema thickness maps, presenting more intuitive 3D morphometry and detailed statistics of retina, CME and SRF compared to the existing unidimensional indicator CRT, supporting more accurate diagnoses and follow-up of DME patients.

#### ACKNOWLEDGEMENTS

**Conflicts of Interest:** Xu JJ, None; Zhou Y, None; Wei QJ, None; Li K, None; Li ZP, None; Yu T, None; Zhao JC, None; Ding DY, None; Li XR, None; Wang GZ, None; Dai H, None.

#### REFERENCES

- 1 International Diabetes Federation. IDF Diabetes Atlas, 9th edition 2019. <http://www.diabetesatlas.org>. Accessed on April 20, 2021.

- 2 Li Y, Teng D, Shi X, *et al.* Prevalence of diabetes recorded in mainland China using 2018 diagnostic criteria from the American Diabetes Association: national cross sectional study. *BMJ* 2020;369:m997.
- 3 Chua J, Lim CXY, Wong TY, Sabanayagam C. Diabetic retinopathy in the Asia-Pacific. *Asia Pac J Ophthalmol (Phila)* 2018;7(1):3-16.
- 4 Miller K, Fortun JA. Diabetic macular edema: current understanding, pharmacologic treatment options, and developing therapies. *Asia Pac J Ophthalmol (Phila)* 2018;7(1):28-35.
- 5 Schmidt-Erfurth U, Garcia-Arumi J, Bandello F, Berg K, Chakravarthy U, Gerendas BS, Jonas J, Larsen M, Tadayoni R, Loewenstein A. Guidelines for the management of diabetic macular edema by the European Society of Retina Specialists (EURETINA). *Ophthalmologica* 2017;237(4):185-222.
- 6 Flaxel CJ, Adelman RA, Bailey ST, Fawzi A, Lim JJ, Vemulakonda GA, Ying GS. Diabetic retinopathy preferred practice pattern®. *Ophthalmology* 2020;127(1):P66-P145.
- 7 Yuan Y, Chen X, Wang J. Object-Contextual Representations for Semantic Segmentation. *Computer Vision–ECCV 2020*; 2020; Cham. Springer International Publishing. [https://link.springer.com/chapter/10.1007/978-3-030-58539-6\\_11](https://link.springer.com/chapter/10.1007/978-3-030-58539-6_11). Accessed on May 20, 2021.
- 8 Wang J, Sun K, Cheng T, Jiang B, Deng C, Zhao Y, Liu D, Mu YD, Tan M, Wang X, Liu W, Xiao B. Deep high-resolution representation learning for visual recognition. *IEEE Trans Pattern Anal Mach Intell* 2021;43(10):3349-3364.
- 9 Sun K, Xiao B, Liu D, *et al.* Deep High-Resolution Representation Learning for Human Pose Estimation. 2019 IEEE/CVF Conference on Computer Vision and Pattern Recognition (CVPR); 15-20 June, 2019. <https://ieeexplore.ieee.org/document/8953615>. Accessed on May 20, 2021.
- 10 Girish GN, Thakur B, Chowdhury SR, Kothari AR, Rajan J. Segmentation of intra-retinal cysts from optical coherence tomography images using a fully convolutional neural network model. *IEEE J Biomed Health Inform* 2019;23(1):296-304.
- 11 Lee CS, Tying AJ, Deruyter NP, Wu Y, Rokem A, Lee AY. Deep-learning based, automated segmentation of macular edema in optical coherence tomography. *Biomed Opt Express* 2017;8(7):3440-3448.
- 12 Ronneberger O. U-Net Convolutional Networks for Biomedical Image Segmentation. *Bildverarbeitung für die Medizin* 2017; 2017; Berlin, Heidelberg. Springer Berlin Heidelberg. <https://arxiv.org/abs/1505.04597>. Accessed on May 20, 2021.
- 13 Roy AG, Conjeti S, Karri SPK, Sheet D, Katouzian A, Wachinger C, Navab N. ReLayNet: retinal layer and fluid segmentation of macular optical coherence tomography using fully convolutional networks. *Biomed Opt Express* 2017;8(8):3627-3642.
- 14 Guo Y, Hormel TT, Xiong H, Wang J, Hwang TS, Jia Y. Automated segmentation of retinal fluid volumes from structural and angiographic optical coherence tomography using deep learning. *Transl Vis Sci Technol* 2020;9(2):54.
- 15 Liu X, Wang S, Zhang Y, Liu D, Hu W. Automatic fluid segmentation in retinal optical coherence tomography images using attention based deep learning. *Neurocomputing* 2021;452:576-591.
- 16 Li MX, Yu SQ, Zhang W, Zhou H, Xu X, Qian TW, Wan YJ. Segmentation of retinal fluid based on deep learning: application of three-dimensional fully convolutional neural networks in optical coherence tomography images. *Int J Ophthalmol* 2019;12(6):1012-1020.
- 17 Hu J, Chen Y, Yi Z. Automated segmentation of macular edema in OCT using deep neural networks. *Med Image Anal* 2019;55:216-227.
- 18 Chen LC, Zhu Y, Papandreou G, *et al.* Encoder-Decoder with Atrous Separable Convolution for Semantic Image Segmentation. *Computer Vision–ECCV 2018*; 2018; Cham. Springer International Publishing. [https://link.springer.com/chapter/10.1007/978-3-030-01234-2\\_49](https://link.springer.com/chapter/10.1007/978-3-030-01234-2_49). Accessed on May 20, 2021.
- 19 Liefers B, Venhuizen FG, Schreur V, van Ginneken B, Hoyng C, Fauser S, Theelen T, Sánchez CI. Automatic detection of the foveal center in optical coherence tomography. *Biomed Opt Express* 2017;8(11):5160-5178.
- 20 Breger A, Ehler M, Bogunovic H, Waldstein SM, Philip AM, Schmidt-Erfurth U, Gerendas BS. Supervised learning and dimension reduction techniques for quantification of retinal fluid in optical coherence tomography images. *Eye (Lond)* 2017;31(8):1212-1220.
- 21 Samagaio G, Estévez A, Moura J, Novo J, Fernández MI, Ortega M. Automatic macular edema identification and characterization using OCT images. *Comput Methods Programs Biomed* 2018;163:47-63.
- 22 Jemshi KM, Gopi VP, Issac Niwas S. Development of an efficient algorithm for the detection of macular edema from optical coherence tomography images. *Int J Comput Assist Radiol Surg* 2018;13(9):1369-1377.
- 23 Schlegl T, Waldstein SM, Bogunovic H, Endstraßer F, Sadeghipour A, Philip AM, Podkowinski D, Gerendas BS, Langs G, Schmidt-Erfurth U. Fully automated detection and quantification of macular fluid in OCT using deep learning. *Ophthalmology* 2018;125(4):549-558.
- 24 Bogunovic H, Venhuizen F, Klimscha S, *et al.* RETOUCH: the retinal OCT fluid detection and segmentation benchmark and challenge. *IEEE Trans Med Imaging* 2019;38(8):1858-1874.
- 25 Niu S, Chen Q, de Sisternes L, Leng T, Rubin DL. Automated detection of foveal center in SD-OCT images using the saliency of retinal thickness maps. *Med Phys* 2017;44(12):6390-6403.
- 26 Wu J, Waldstein SM, Montuoro A, Gerendas BS, Langs G, Schmidt-Erfurth U. Automated fovea detection in spectral domain optical coherence tomography scans of exudative macular disease. *Int J Biomed Imaging* 2016;2016:7468953.